



Published in final edited form as:

Am J Trop Med Hyg. 2006 April ; 74(4): 568–572.

DIAGNOSIS OF MALARIA BY MAGNETIC DEPOSITION MICROSCOPY

PETER A. ZIMMERMAN^{*}, JODI M. THOMSON, HISASHI FUJIOKA, WILLIAM E. COLLINS,
and MACIEJ ZBOROWSKI

Case Western Reserve University, Center for Global Health and Diseases, Cleveland, Ohio;
Case Western Reserve University, Institute of Pathology, Cleveland, Ohio; Centers for Disease
Control and Prevention, Division of Parasitic Diseases, Chamblee, Georgia; The Cleveland Clinic
Foundation, Department of Biomedical Engineering/Lerner Research Institute, Cleveland, Ohio

Abstract

Although malaria contributes to a significant public health burden, malaria diagnosis relies heavily on either non-specific clinical symptoms or blood smear microscopy methods developed in the 1930s. These approaches severely misrepresent the number of infected individuals and the reservoir of parasites in malaria-endemic communities and undermine efforts to control disease. Limitations of conventional microscopy-based diagnosis center on time required to examine slides, time required to attain expertise sufficient to diagnose infection accurately, and attrition from the limited number of existing malaria microscopy experts. Earlier studies described magnetic properties of *Plasmodium falciparum* but did not refine methods to diagnosis infection by all four human malaria parasite species. Here, following specific technical procedures, we show that it is possible to concentrate all four human malaria parasite species, at least 40-fold, on microscope slides using very inexpensive magnets through an approach termed magnetic deposition microscopy. This approach delivered greater sensitivity than a thick smear preparation while maintaining the clarity of a thin smear to simplify species-specific diagnosis. Because the magnetic force necessary to concentrate parasites on the slide is focused at a precise position relative to the magnet surface, it is possible to examine a specific region of the slide for parasitized cells and avoid the time-consuming process of scanning the entire slide surface. These results provide insight regarding new strategies for performing malaria blood smear microscopy.

INTRODUCTION

Progress against malaria through mosquito control efforts using dichloro-diphenyl-trichloroethane (DDT) and effective chloroquine-based parasite treatment made significant strides in areas where primary health care and administrative and financial support for malaria eradication efforts have been available.¹ However, in many developing tropical countries, socio-economic factors in combination with selection of insecticide-resistant mosquitoes and drug-resistant parasites arose as challenges to the World Health

Copyright © 2006 by The American Society of Tropical Medicine and Hygiene

^{*}Address correspondence to: Peter A. Zimmerman, Center for Global Health and Diseases, Case Western Reserve University School of Medicine, Wolstein Research Building, 4-125, Cleveland, OH 44106-7286. paz@case.edu.

Authors' addresses: Peter A. Zimmerman and Jodi M. Thomson, Center for Global Health and Diseases, Case Western Reserve University School of Medicine, Wolstein Research Building, 4-125, Cleveland, OH 44106-7286. Hisashi Fujioka, Institute of Pathology, Case Western Reserve University School of Medicine and University Hospitals of Cleveland, Cleveland, OH 44106-4907. William E. Collins, Division of Parasitic Diseases, National Center for Infectious Diseases, Centers for Disease Control and Prevention, 4770 Buford Highway, Chamblee, GA 30341. Maciej Zborowski, Department of Biomedical Engineering, Lerner Research Institute, The Cleveland Clinic Foundation, 9500 Euclid Avenue, Cleveland, OH 44195.

Reprint requests: Peter A. Zimmerman, Center for Global Health and Diseases, Case Western Reserve University School of Medicine, Wolstein Research Building, 4-125, Cleveland, OH 44106-7286. paz@case.edu.

Organization–supported malaria eradication program² that was terminated in 1969.³ With a limited arsenal of effective antimalarial drugs and continuing struggles to develop vaccines against any of the human *Plasmodium* parasite species, malaria control efforts have stalled. Today, malaria continues to be a major global health threat, causing 300–500 million infections and 1–2 million deaths annually.^{4,5}

An important impediment to effective malaria treatment and control is the absence of low-cost diagnostic tools and strategies capable of evaluating infection status rapidly in rural settings where the majority of malaria cases are encountered. As a result, generalized treatment of malarial and bacterial infections follows symptom-based diagnosis.⁴ This approach is certain to contribute to selection favoring drug-resistant parasites and bacteria. Although the conventional blood smear serves as the “gold standard” tool for malaria diagnosis (individual diagnosis ≈ US\$0.12–0.40),⁴ it is widely acknowledged that molecular tools are faster (antigen-based rapid diagnostic tools [RDTs])^{6,7} or provide significantly greater sensitivity and specificity (polymerase chain reaction [PCR]).^{8–10} However, molecular techniques are unlikely to become “gold standard” malaria diagnostic methods. Current antigen-based RDTs are expensive (individual diagnosis ≈ US\$0.60–2.50),⁴ do not assess *Plasmodium vivax*, *P. malariae*, or *P. ovale* with specificity, and have been observed to be less sensitive than the blood smear.^{4,11} PCR-based diagnosis (individual diagnosis ≈ US\$0.50–1.00)⁴ requires a laboratory with electricity and expensive equipment and is most expedient when analysis is performed on large numbers of samples in a 96-well plate format.¹²

In an attempt to overcome some problems inherent to blood smear microscopy, we have developed a magnet-based approach to concentrate malaria parasites and augment detection of malaria-infected erythrocytes by microscopy. This system, malaria magnetic deposition microscopy (MDM), exploits the fact that *Plasmodium* species parasites produce a crystalline by-product, hemozoin, from heme liberated during hemoglobin digestion. Unlike previous systems requiring elution of cells from steel mesh,^{13,14} MDM captures parasitized erythrocytes in a narrow magnetic field and deposits them directly onto a small region of a polyester slide, which is immediately ready for fixation and staining. By concentrating parasites, MDM increases the sensitivity of diagnosis and decreases the time it takes to read the slide. Here we show the ability of MDM to concentrate parasites of all four human malaria parasite species, including efficient capture of *P. falciparum* gametocytes.

MATERIALS AND METHODS

Parasite sources

Blood for this study was obtained from primates at the Centers for Disease Control and Prevention (CDC) Division of Parasitic Diseases, Atlanta, GA, and Yerkes National Primate Research Center, Atlanta, GA. *P. falciparum*-infected blood was drawn from an *Aotus nancymai* monkey with a peripheral blood parasitemia of 2.7%. *P. vivax*- and *P. malariae*-infected blood samples were drawn from *Aotus vociferans* monkeys with peripheral blood parasitemias of 0.1% and 0.4%, respectively. *P. ovale*-infected blood was taken from a chimpanzee (*Pan troglodytes*) with a parasitemia of 0.2%. All infected primate blood donors in the study had been splenectomized. Blood was collected in heparin tubes and diluted 1:6 with phosphate-buffered saline (PBS), pH 7.2, before loading 500 μL of the diluted sample into the syringe pump. To produce a *P. falciparum*/*P. vivax* mixed infection, equal volumes of whole blood from each infection were mixed and immediately diluted 1:6 with PBS. All samples were processed fresh, within 6 hours of the time that blood samples were drawn. Protocols for infecting monkeys with malaria parasites were approved by the CDC Institutional Animal Care and Use Committee according to Public Health Service Policy.

Malaria MDM device specifications

Malaria MDM is based on an open-gradient magnetic field separator and a thin-film magnetapheresis process developed for cell analysis during past studies.^{15–19} The magnetic field was designed to maximize local Maxwell stress gradients that drive cell separation from the flowing suspension (Figure 1A), optimizing erythrocyte capture from the cell suspension.²⁰ A fringing field of an interpolar gap, combined with a thin flow channel pressed against the interpolar gap, was used as a means of cell capture from suspension. The magnetic field was generated by a permanent magnet assembly comprising ferrite magnets (Dexter Magnetic Technologies, Elk Grove Village, IL) and a pair of 1016 low-carbon steel pole pieces (in-house model C designation).¹⁵ The interpolar gap width was 1.27 mm; the magnetic field strength, H , measured at the midline of the interpolar gap at the magnet surface was 1.135×10^6 A/m; the magnetic field intensity, B , was 1.426 T; the magnetic field gradient was 804 T/m, and the magnitude of the Maxwell stress gradient was 1.824×10^9 AT/m². The direction of the resulting magnetic force acting on erythrocytes was essentially perpendicular to the deposition surface along the width of the interpolar gap, and its magnitude rapidly decreased with distance from the interpolar gap (Figure 1A). The flow channel lumen (6.4 mm \times 0.25 mm), including sample inlet and outlet tubing, was formed to meet a cutout in a silicone rubber gasket separating a thin, inner polyester sheet (75 μ m thick or one half the thickness of no. 1 glass coverslips, Clear Polyester; McMaster-Carr, Aurora, OH) from a thick, outer acrylic cover (4 mm). The interpolar gap formed a magnetic barrier to malaria-infected cells and was sufficiently long to accommodate five flow channels. Cell suspensions (500 μ L each) were delivered in a continuous manner into flow channels by syringes connected to inlet tubing and evacuated from flow channels by outlet tubing leading to waste containers (Figure 1B). All five samples were held in 1-mL sterile disposable syringes (Becton-Dickenson, Franklin Lakes, NJ) mounted on the syringe pump (Sage Instruments, Cambridge, MA). Each syringe was connected to its matching flow chamber through a 1,000- μ L pipette tip, 10-mm-long Tygon tubing (inner diameter [ID] 1.59 mm; outer diameter, [OD] 3.18 mm; Norton Performance Plastic Co., Akron, OH), and 60-mm-long Teflon tubing (ID 0.79 mm, OD 1.59 mm; [Zeus Inc., Boise, ID]). The same type Teflon tubing carried eluate fractions to sample collection tubes. The syringe pump was modified by fitting it with a five-syringe receptacle and by extending a pusher plate (not pictured) to accommodate all five syringe plungers. The position of each plunger relative to the pusher plate was individually adjusted by thumb screws to allow simultaneous delivery of all five samples. Before each experiment, the flow chambers and connecting tubings were primed with PBS (pH 7.2) so that cells entered the magnetic deposition zone in a fully developed flow. The flow channel dimensions and the volumetric flow rate of the cell sample were selected to maximize the cell interaction with the magnetic field, and consequently, increase the likelihood of depositing mobile cells magnetophoretically on the thin plastic sheet surface. The flow channel cross-section was 6.4 mm \times 0.25 mm, the volumetric flow rate was 0.7 mL/h, the resulting average linear velocity of fluid across the interpolar gap region was 1.2 mm/s, and the average fluid volume element residence time in the interpolar gap region (taken as twice the interpolar gap width or 2.54 mm) was approximately 2 seconds.

After the entire cell suspension volume was pumped across the fringing field of the interpolar gap, the flow channel was disassembled, and the plastic sheet was evaluated for the presence of cells in the area exposed to the fringing field. The resulting, expected deposition pattern of infected erythrocytes formed a well-defined band on the plastic sheet visible by an unaided eye approximating the breadth of the flow channel and the width of the interpolar gap (Figure 1, B and C).

Staining and microscopy

Cells captured on the polyester slides were fixed for 30 seconds in 100% methanol and subsequently stained with 4% Giemsa. Once dried, the slides were mounted between a standard glass slide and coverslip with Permount (Fisher Scientific, Pittsburgh, PA). The slides were visualized and photographed under oil immersion at $\times 100$ power.

RESULTS AND DISCUSSION

We used MDM to concentrate erythrocytes parasitized by all four human malaria species (Figure 2). *P. falciparum*-infected blood samples were enriched 40-fold from a parasitemia of 2.7% (Figure 2A) to nearly 100% (Figure 2B). *P. vivax*-infected blood samples were enriched up to 250-fold, from an initial parasitemia of 0.1% (Figure 2C) to clusters with 25% (Figure 2D) infected erythrocytes. *P. malariae*-infected blood samples were enriched from 0.4% to 100% infected erythrocytes, at least a 250-fold concentration (Figure 2, E and F). *P. ovale*-infected blood samples were enriched up to 375-fold from an initial parasitemia of 0.2% to clusters containing 75% infected erythrocytes (Figure 2, G and H). Additionally, we observed that MDM successfully concentrated *P. simium*-infected erythrocytes (data not shown). This observation, along with earlier reports, where magnetic columns were used to enrich murine malaria parasite (*P. berghei*) ookinetes,²¹ suggests that magnetic capture methods are generally applicable to *Plasmodium* species.

In most malarious regions of the world, multiple *Plasmodium* species are present in the population,²² and mixed-species infections within individuals are common.¹² Therefore, to determine how a mixed *Plasmodium* species infection would be evaluated by malaria MDM analysis, we performed a mixing experiment with *P. falciparum*- and *P. vivax*-infected blood samples (equal volumes of each sample) and prepared slides, and evaluated the mixture as previously described for the unmixed samples. In our results shown in Figure 3, we provide evidence to show that malaria MDM concentrated infected cells of both *Plasmodium* species on one slide. Additionally, *P. falciparum*- and *P. vivax*-infected erythrocytes seem to have been captured in proportions similar to the initial parasitemia (~20:1).

Consistent with hemoglobin digestion, liberation, and crystallization of free heme into hemozoin, we observed that trophozoites, schizonts, and gametocytes of all species were captured by MDM, but there was a noticeable under-representation of ring stage parasites. This observation is consistent with earlier reports and our own recent studies, where infected erythrocytes containing mature trophozoites and schizonts were captured on a magnetized steel mesh, whereas ring-stage parasites were less susceptible to the magnetic field.^{13,14,23} This is an important limitation of the current method. Diagnosis of *P. falciparum* infection relies on observation of rings owing to the sequestration of trophozoites and schizonts in post-capillary venules away from peripheral blood flow ordinarily monitored by vena puncture or finger prick blood collection techniques. Moreover, because parasitemia is known to fluctuate at regular intervals, and the early developmental stages can comprise the majority of infected erythrocytes, capture of ring and early trophozoites would greatly improve the ability to estimate parasitemia. With the enrichment of gametocytes, it may be possible to estimate better gametocytemia and evaluate malaria transmission potential within endemic populations. Finally, we observed that hemozoin-laden macrophages were also captured by MDM from *P. falciparum*-infected blood (Figures 2B and 3).

As can be observed in Figures 2 and 3, clustering of cells can compress erythrocyte membranes; however, this did not distort parasite morphology, staining, or infected versus un-infected erythrocyte size characteristics familiar to malaria microscopists. Slides from samples with lower parasitemia tend to have smaller and fewer cell clusters than high level

infections. Unlike the typical blood smear pattern of evenly spaced cells, MDM deposits infected erythrocytes in cell clusters (uninfected erythrocytes can be found within these clusters at low frequencies) in close proximity to the inter-polar gap region between the edges of the magnetic bars (Figure 1). This greatly assists microscopists in locating infected cells and in restricting the region of the slide to be evaluated. Additionally, because MDM enriches capture of parasitized erythrocytes, it should facilitate differentiation of species- and stage-specific morphologic features by providing opportunity for comparison among a greater number of infected cells. These characteristics of malaria MDM slide preparations should contribute to more rapid evaluation of blood slides. Similarly, we anticipate that malaria MDM will also contribute to more thorough and efficient teaching of microscopy-based malaria diagnosis.

In conclusion, we showed how malaria MDM enriches capture of parasitized erythrocytes and macrophages containing hemozoin. From these observations, it may be possible to guide development of future magnet-based strategies to label ring and early trophozoite cell surface proteins and capture these stages as efficiently as hemozoin-containing trophozoites, schizonts, and gametocytes. Because our current studies used infected blood samples from splenectomized non-human primates, it will be important to determine the efficiency with which malaria MDM captures *Plasmodium*-infected erythrocytes from infected people in different malaria endemic regions of the world. In preparation for field testing, we developed a prototype MDM device that requires no electricity and fits easily within a 45 mm × 45 mm × 105-mm box (500 g). Because the magnets involved in this technology are very inexpensive, we anticipate that costs associated with malaria MDM diagnosis will be equal to conventional blood smear microscopy (individual diagnosis ≈ US\$0.12–0.40).⁴ This approach may facilitate field-based malaria diagnosis and improve the specificity of health care in developing tropical countries. Application of such methods could contribute to significant reduction in malaria infection and containing anti-malarial drug resistance. Finally, malaria MDM could also be used to enhance laboratory-based studies attempting to characterize factors that limit *P. falciparum* invasion of erythrocytes and efforts to develop new anti-malarial drugs and vaccines.

Acknowledgments

The authors thank Boris Kligman, JoAnn Sullivan, and Kiet Luc for technical assistance and David McNamara and Laurin Kasehagen for helpful comments and criticisms during the preparation of the manuscript.

Financial support: This work was supported by NIH AI46919, AI52312 (P. A. Zimmerman), and CA62349 (M. Zborowski.). J. M. Thomson was supported in part by NIH T32 GM07250 and the Case Medical Scientist Training Program.

References

1. Bruce-Chwatt, LJ. Essential Malariology. London: William Heinemann Medical Books; 1985.
2. World Health Organization. Malaria: Sixth Report of the Expert Committee. Geneva: World Health Organization; 1957.
3. World Health Organization. Re-examination of the Global Strategy of Malaria Eradication. Geneva: World Health Organization; 1969.
4. New Perspectives in Malaria Diagnosis. Geneva: World Health Organization; 2000.
5. Snow RW, Guerra CA, Noor AM, Myint HY, Hay SI. The global distribution of clinical episodes of *Plasmodium falciparum* malaria. *Nature*. 2005; 434:214–217. [PubMed: 15759000]
6. Shiff CJ, Premji Z, Minjas JN. The rapid manual Para-Sight-F test. A new diagnostic tool for *Plasmodium falciparum* infection. *Trans R Soc Trop Med Hyg*. 1993; 87:646–648. [PubMed: 8296363]

7. Palmer CJ, Lindo JF, Klaskala WI, Quesada JA, Kaminsky R, Baum MK, Ager AL. Evaluation of the OptiMAL test for rapid diagnosis of *Plasmodium vivax* and *Plasmodium falciparum* malaria. *J Clin Microbiol.* 1998; 36:203–206. [PubMed: 9431947]
8. Snounou G, Viriyakosol S, Zhu XP, Jarra W, Pinheiro L, do Rosario VE, Thaithong S, Brown KN. High sensitivity of detection of human malaria parasites by the use of nested polymerase chain reaction. *Mol Biochem Parasitol.* 1993; 61:315–320. [PubMed: 8264734]
9. Mehlotra RK, Lorry K, Kastens W, Miller SM, Alpers MP, Bockarie M, Kazura JW, Zimmerman PA. Random distribution of mixed species malaria infections in Papua New Guinea. *Am J Trop Med Hyg.* 2000; 62:225–231. [PubMed: 10813477]
10. McNamara DT, Thomson JM, Kasehagen LJ, Zimmerman PA. Development of a multiplex PCR-ligase detection reaction assay for diagnosis of infection by the four parasite species causing malaria in humans. *J Clin Microbiol.* 2004; 42:2403–2410. [PubMed: 15184411]
11. Moody A. Rapid diagnostic tests for malaria parasites. *Clin Microbiol Rev.* 2002; 15:66–78. [PubMed: 11781267]
12. Zimmerman PA, Mehlotra RK, Kasehagen LJ, Kazura JW. Why do we need to know more about mixed *Plasmodium* species infections in humans? *Trends in Parasitology.* 2004; 20:440–447. [PubMed: 15324735]
13. Paul F, Roath S, Melville D, Warhurst DC, Osisanya JO. Separation of malaria-infected erythrocytes from whole blood: use of a selective high-gradient magnetic separation technique. *Lancet.* 1981; 2:70–71. [PubMed: 6113443]
14. Nalbandian RM, Sammons DW, Manley M, Xie L, Sterling CR, Egen NB, Gingras BA. A molecular-based magnet test for malaria. *Am J Clin Pathol.* 1995; 103:57–64. [PubMed: 7817946]
15. Fang B, Zborowski M, Moore LR. Detection of rare MCF-7 breast carcinoma cells from mixtures of human peripheral leukocytes by magnetic deposition analysis. *Cytometry.* 1999; 36:294–302. [PubMed: 10404144]
16. Zborowski M, Fuh CB, Green R, Baldwin NJ, Reddy S, Douglas T, Mann S, Chalmers JJ. Immunomagnetic isolation of magnetoferritin-labeled cells in a modified ferrograph. *Cytometry.* 1996; 24:251–259. [PubMed: 8800558]
17. Zborowski M, Fuh CB, Green R, Sun L, Chalmers JJ. Analytical magnetapheresis of ferritin-labeled lymphocytes. *Anal Chem.* 1995; 67:3702–3712. [PubMed: 8644920]
18. Zborowski M, Malcheski PS, Savon SR, Green R, Holl GS, Nose Y. Modification of ferrography method for analysis of lymphocytes and bacteria. *Wear.* 1991; 142:135–149.
19. Zborowski M, Malcheski PS, Jan TF, Hall GS. Quantitative separation of bacteria in saline solution using lanthanide Er(III) and a magnetic field. *J Gen Microbiol.* 1992; 138:63–68. [PubMed: 1556557]
20. Zborowski, M. Physics of the magnetic cell sorting. In: Hafeli, U.; Schutt, W.; Teller, J.; Zborowski, M., editors. *Scientific and Clinical Applications of Magnetic Microcarriers: An Overview.* New York: Plenum Press; 1997. p. 205-231.
21. Carter V, Cable HC, Underhill BA, Williams J, Hurd H. Isolation of *Plasmodium berghei* ookinetes in culture using Nycodenz density gradient columns and magnetic isolation. *Malar J.* 2003; 2:35. [PubMed: 14613512]
22. Snounou G, White NJ. The co-existence of *Plasmodium*: sidelights from falciparum and vivax malaria in Thailand. *Trends Parasitol.* 2004; 20:333–339. [PubMed: 15193565]
23. Moore LR, Fujioka H, Williams PS, Chalmers JJ, Grimberg BT, Zimmerman PA, Zborowski M. Hemoglobin degradation in malaria-infected erythrocytes determined from live cell magnetophoresis. *FASEB J.* 2006 (in press).

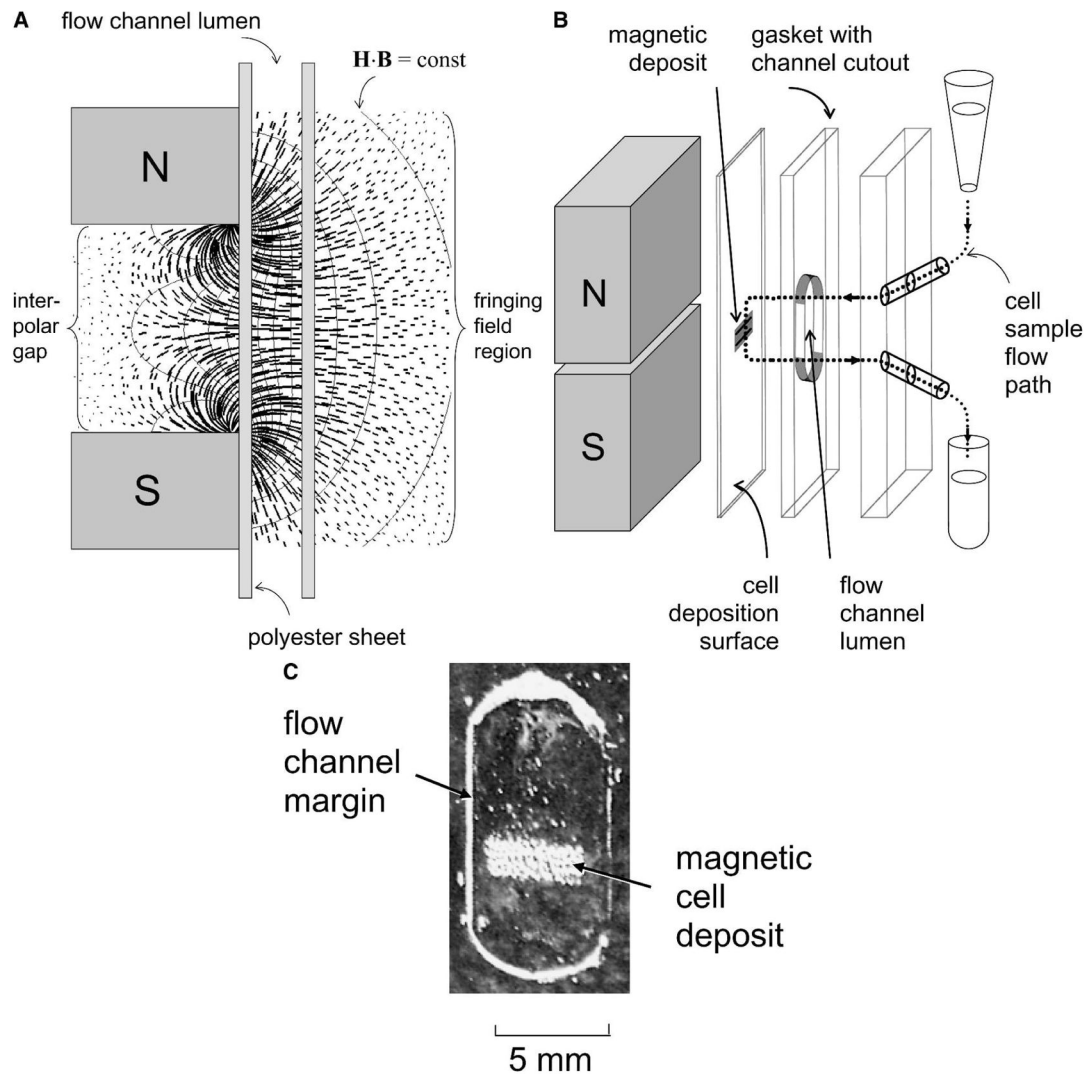


Figure 1. Physical principles of malaria MDM. **(A)** Magnetic field and cell path lines of the thin-film magnetapheresis device used for erythrocyte deposition. The quantity $H \cdot B$ indicates Maxwell stress isoline, where H is the magnetic field strength and B is the magnetic field intensity (or flux density); N, north; S, south. The magnetically susceptible erythrocytes follow a path (thick) along the Maxwell stress gradients (in the direction perpendicular to the Maxwell stress isolines). Note concentration of path lines at the inter-polar gap area between the pole piece tips resulting in a highly localized erythrocyte capture pattern on the polyester sheet surface. The convective and sedimentation effects inside the channel lumen were omitted for clarity. The inter-polar gap, the flow channel lumen, and the polyester sheet thickness are drawn to scale; acrylic cover not drawn to scale. **(B)** Components of the malaria MDM device and the sample flow path (\rightarrow ; exploded view). Note the position of the erythrocyte deposition band next to the magnet pole piece tips, represented diagrammatically, resulting from action of the magnetic field **(A)**. Five such modules were integrated into a single MDM apparatus. Drawing is not to scale. **(C)** An unaided eye appearance of the magnetic deposition, collected in the inter-polar gap area **(A and B)** from a *P. falciparum*-parasitized blood sample.

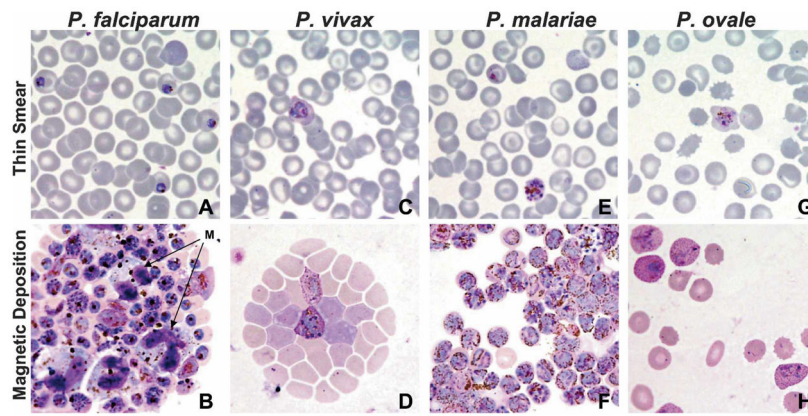


Figure 2. Malaria MDM concentrates *Plasmodium*-infected erythrocytes. *P. falciparum* (A and B), *P. vivax* (C and D), *P. malariae* (E and F), and *P. ovale* (G and H) infections comparing conventional thin blood smear (top) and malaria MDM (bottom) for each *Plasmodium* species were prepared from infected non-human primate blood samples. Individual parasitemias determined by the Earle and Perez method were 2.7% for *P. falciparum*, 0.1% for *P. vivax*, 0.4% for *P. malariae*, and 0.2% for *P. ovale*. All slides were stained using standard Giemsa staining procedures and examined using a $\times 100$ oil immersion objective. In B, M = macrophage.

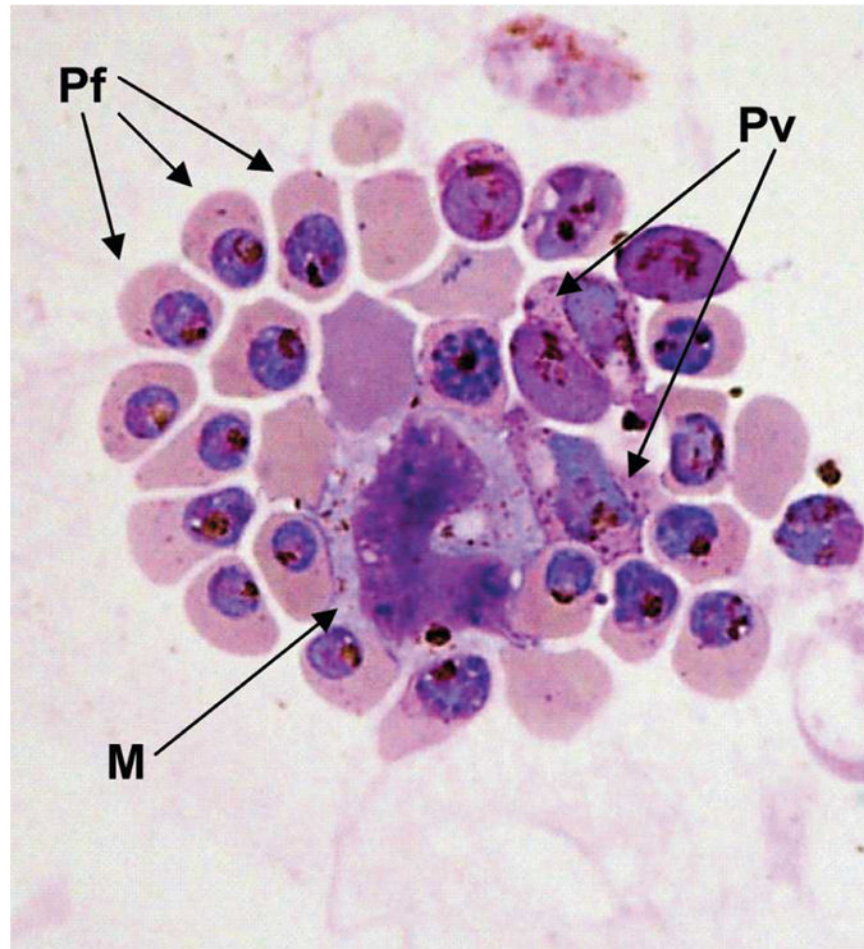


Figure 3. MDM detection of *P. falciparum* and *P. vivax* from a mixed blood sample. Equal volumes of blood from *P. falciparum*–(initial parasitemia of 2.7%) and *P. vivax*– (initial parasitemia of 0.1%) infected monkeys were mixed and subjected to MDM analysis. Giemsa stained slides show MDM concentration of *P. falciparum* (Pf), *P. vivax* (Pv), and macrophages (M) containing hemozoin.